

Ghost-gluon running coupling, power corrections, and the determination of $\Lambda_{\overline{\text{MS}}}$ Ph. Boucaud,¹ F. De Soto,² J. P. Leroy,¹ A. Le Yaouanc,¹ J. Micheli,¹ O. Pène,¹ and J. Rodríguez-Quintero³¹*Laboratoire de Physique Théorique et Hautes Energies* Université de Paris XI, Bâtiment 211, 91405 Orsay Cedex, France*²*Dpto. Sistemas Físicos, Químicos y Naturales, Universidad Pablo de Olavide, 41013 Sevilla, Spain.*³*Dpto. Física Aplicada, Fac. Ciencias Experimentales, Universidad de Huelva, 21071 Huelva, Spain.*

(Received 14 November 2008; published 23 January 2009)

We compute a formula including operator-product expansion power corrections to describe the running of a QCD coupling nonperturbatively defined through the ghost and gluon dressing functions. This turns out to be rather accurate. We propose the “plateau” procedure to compute $\Lambda_{\overline{\text{MS}}}$ from the lattice computation of the running coupling constant. We show a good agreement between the different methods which have been used to estimate $\Lambda_{\overline{\text{MS}}}^{N_f=0}$. We argue that $\Lambda_{\overline{\text{MS}}}$ or the strong coupling constant computed with different lattice spacings may be used to estimate the lattice spacing ratio.

DOI: 10.1103/PhysRevD.79.014508

PACS numbers: 12.38.Gc, 11.15.Ha, 12.38.Aw, 12.38.Cy

I. INTRODUCTION

Much work has been devoted in the last years to the study of the QCD running coupling constant determined from lattice simulations, in its perturbative regime [1–9] as well as in the deep infrared domain [10]. The two main approaches to obtain the running coupling in terms of the renormalization momentum were either an application of the Schrödinger functional method with special boundary conditions or the confrontation of the behavior with respect to the renormalization scale of 2-gluon and 3-gluon Green functions with the corresponding perturbative predictions. The latter Green’s functions approach also revealed a dimension-two nonzero gluon condensate in the Landau gauge. Much work has been also done to investigate its phenomenological implications in the gauge-invariant world [11]. In a very recent work [9], the Green’s function approach to estimate $\Lambda_{\overline{\text{MS}}}$ has been pursued by exploiting a nonperturbative definition of the coupling derived from the ghost-gluon vertex and computed over a large momentum window in the perturbative regime. Much of this work was based on the analysis of *quenched* lattice simulations and led to the determination of $\Lambda_{\overline{\text{MS}}}$ in pure Yang-Mills ($N_f = 0$). Works on *unquenched* lattice configurations ($N_f = 2$) started some time ago [12] and have been more actively pursued recently.

Many unquenched configurations are presently available and we are planning to apply what we have learned on pure Yang-Mills to gauge configurations with twisted $N_f = 2$ [13] and $N_f = 2 + 1 + 1$ dynamical quarks. Thus, a very realistic estimate of $\Lambda_{\overline{\text{MS}}}$, directly comparable with experimental determinations, will become an immediate possibility. With the latter remarks in mind, we pay attention in this paper to study of the above-mentioned nonperturbative coupling derived from the ghost-gluon vertex. We show in Sec. II that, when the incoming ghost momentum van-

ishes—and only in this case—this ghost-gluon vertex can be directly related to the bare gluon and ghost propagators; we then obtain a formula to describe its running including nonperturbative power corrections. We propose to confront this formula with lattice estimates of the coupling and we argue that this constitutes an optimal method for the identification of $\Lambda_{\overline{\text{MS}}}$ and of the gluon condensate. In particular, it benefits from two main advantages: it has only a two-points function to deal with (much simpler to be managed and more precise than a three-points function) and the precision could be improved by extending the analysis of lattice data over a very large momenta window. In Sec. III, we apply this procedure to previously published lattice data for quenched simulations with a two-sided goal: (i) to check the method and (ii) to confirm the consistency of the picture we have acquired for the UV behavior of Green functions in pure Yang-Mills. We finally conclude in Sec. IV and add two appendices for presenting the gluon and ghost anomalous dimension coefficients in the momentum subtraction scheme (MOM) up to four loops (Appendix A) and the subleading Wilson coefficient up to leading logarithms of ghost and gluon propagators (Appendix B).

II. THE GHOST-GLUON COUPLING

There is a large number of possibilities to define the QCD renormalized coupling constant, depending on the observable used to measure it and on the renormalization scheme. Actually, any observable which behaves, from the perturbative point of view, as g provides a suitable definition for it. Among such quantities stand the 3-gluon and the ghost-gluon vertices, which have been widely used by the lattice community to get a direct knowledge of α_s from simulations. Of course an important criterion to choose among those definitions will be how easy it is to connect it to other commonly used definitions, specially the $\overline{\text{MS}}$ one, and to extract from it fundamental parameters like Λ_{QCD} .

A convenient class of renormalization schemes to work with on the lattice is made of the so-called MOM schemes

*Unité Mixte de Recherche 8627 du Centre National de la Recherche Scientifique.

which are defined through the requirement that a given scalar coefficient function of the Green's function under consideration takes its tree-level value in a specific kinematical situation given up to an overall renormalization scale. To make the point clearer we recall two schemes which we have used in previous works on α_s :

- (i) The symmetric 3-gluon scheme in which one uses the 3-gluon vertex $\Gamma_{\mu\nu\rho}(p_1, p_2, p_3)$ with $p_1^2 = p_2^2 = p_3^2 = \mu^2$.
- (ii) The asymmetric 3-gluon scheme ($\widetilde{\text{MOM}}$) in which the 3-gluon vertex $\Gamma_{\mu\nu\rho}(p_1, p_2, p_3)$ is used with $p_1^2 = p_2^2 = \mu^2, p_3^2 = 0$.

In the present paper we shall apply a specific MOM-type renormalization scheme defined by fixing the (ghost and gluon) propagators and the ghost-gluon vertex at the renormalization point. Let us start by writing the ghost and gluon propagators in Landau gauge as follows:

$$(G^{(2)})_{\mu\nu}^{ab}(p^2, \Lambda) = \frac{G(p^2, \Lambda)}{p^2} \delta_{ab} \left(\delta_{\mu\nu} - \frac{p_\mu p_\nu}{p^2} \right), \quad (1)$$

$$(F^{(2)})^{a,b}(p^2, \Lambda) = -\delta_{ab} \frac{F(p^2, \Lambda)}{p^2},$$

Λ being some regularization parameter ($a^{-1}(\beta)$ if, for instance, we specialize to lattice regularization). The renormalized dressing functions G_R and F_R are defined through

$$G_R(p^2, \mu^2) = \lim_{\Lambda \rightarrow \infty} Z_3^{-1}(\mu^2, \Lambda) G(p^2, \Lambda) \quad (2)$$

$$F_R(p^2, \mu^2) = \lim_{\Lambda \rightarrow \infty} \tilde{Z}_3^{-1}(\mu^2, \Lambda) F(p^2, \Lambda),$$

with renormalization condition

$$G_R(\mu^2, \mu^2) = F_R(\mu^2, \mu^2) = 1. \quad (3)$$

Now, we will consider the ghost-gluon vertex which could be nonperturbatively obtained through a three-point Green function, defined by two ghost and one gluon fields, with amputated legs after dividing by two ghost and one gluon propagators. This vertex can be written quite generally as

$$\begin{aligned} \tilde{\Gamma}_\nu^{abc}(-q, k; q-k) &= \frac{1}{k} \rightarrow \text{diagram} \rightarrow \frac{1}{q} \\ &= i g_0 f^{abc} (q_\nu H_1(q, k) \\ &\quad + (q-k)_\nu H_2(q, k)), \end{aligned} \quad (4)$$

where q is the outgoing ghost momentum and k the incoming one, and renormalized according to

$$\tilde{\Gamma}_R = \tilde{Z}_1 \Gamma. \quad (5)$$

The vertex Γ_ν involves two independent scalar functions. In the MOM renormalization procedure \tilde{Z}_1 is fully determined by demanding that one specific combination of those two form factors (chosen at one's will) be equal to

its tree-level value for a specific kinematical configuration. We choose to apply a MOM prescription for the scalar function $H_1 + H_2$ that multiplies q_ν in Eq. (4) and the renormalization condition reads¹

$$\begin{aligned} (H_1^R(q, k) + H_2^R(q, k))|_{q^2=\mu^2} &= \lim_{\Lambda \rightarrow \infty} \tilde{Z}_1(\mu^2, \Lambda) (H_1(q, k; \Lambda) \\ &\quad + H_2(q, k; \Lambda))|_{q^2=\mu^2} \\ &= 1, \end{aligned} \quad (6)$$

where we prescribe a kinematics for the subtraction point such that the outgoing ghost momentum is evaluated at the renormalization scale, while the incoming one k depends on the choice of several possible configurations; for instance: $k^2 = (q-k)^2 = \mu^2$ (symmetric configuration) or $k=0, (q-k)^2 = \mu^2$ (asymmetric ghost configuration).

On the other hand, the fields involved in the nonperturbative definition of the vertex Γ_ν in Eq. (4) can be directly renormalized by their renormalization constants Z_3 and \tilde{Z}_3 , and the same MOM prescription applied to the scalar combination $H_1 + H_2$ also implies

$$\begin{aligned} g_R(\mu^2) &= \lim_{\Lambda \rightarrow \infty} \tilde{Z}_3(\mu^2, \Lambda) Z_3^{1/2}(\mu^2, \Lambda) g_0(\Lambda^2) (H_1(q, k; \Lambda) \\ &\quad + H_2(q, k; \Lambda))|_{q^2=\mu^2} \\ &= \lim_{\Lambda \rightarrow \infty} g_0(\Lambda^2) \frac{Z_3^{1/2}(\mu^2, \Lambda^2) \tilde{Z}_3(\mu^2, \Lambda^2)}{\tilde{Z}_1(\mu^2, \Lambda^2)}. \end{aligned} \quad (7)$$

We combine both Eq. (6) and the first-line equation of (7) to replace $H_1 + H_2$ and obtain the second line that shows the well-known relationship $Z_g = (Z_3^{1/2} \tilde{Z}_3)^{-1} \tilde{Z}_1$, where $g_R = Z_g^{-1} g_0$.

We turn now to the specific MOM-type renormalization scheme defined by a *zero incoming ghost momentum*. Since those kinematics are the ones (and the only ones) in which Taylor's well-known nonrenormalization theorem (cf. Ref. [14]) is valid we shall refer to this scheme as to the T scheme and the corresponding quantities will bear a T subscript. Then, in Eq. (4), we set k to 0 and get

$$\tilde{\Gamma}_\nu^{abc}(-q, 0; q) = i g_0 f^{abc} (H_1(q, 0) + H_2(q, 0)) q_\nu. \quad (8)$$

Now, Taylor's theorem states that $H_1(q, 0; \Lambda) + H_2(q, 0; \Lambda)$ is equal to 1 in full QCD for any value of q . Therefore, the renormalization condition Eq. (6) implies $\tilde{Z}_1(\mu^2) = 1$ and then

$$\alpha_T(\mu^2) \equiv \frac{g_T^2(\mu^2)}{4\pi} = \lim_{\Lambda \rightarrow \infty} \frac{g_0^2(\Lambda^2)}{4\pi} G(\mu^2, \Lambda^2) F^2(\mu^2, \Lambda^2), \quad (9)$$

where we also apply the renormalization condition for the

¹In the case of zero-momentum gluon, an appropriate choice would be $\tilde{Z}_1(\mu^2) H_1(q, q)|_{q^2=\mu^2} = 1$. This would make the renormalized vertex equal to its tree-level value at the renormalization scale.

propagators Eqs. (2) and (3) to replace the renormalization constants Z_3 and \tilde{Z}_3 by the bare dressing functions. The remarkable feature of Eq. (9) is that it involves only F and G so that no measure of the ghost-gluon vertex is needed for the determination of the coupling constant.

Equation (9) has extensively been advocated and studied on the lattice (see for instance Ref. [15]) and used for a determination of Λ_{QCD} in Ref. [9]. However it must be stressed that the T scheme is the *only* one in which $\tilde{Z}_1 = 1$. In any other scheme \tilde{Z}_1 will be finite (since going from one scheme to any other one only involves an additional finite renormalization) but will keep a nontrivial dependence on the scale, in particular, for the symmetric scheme of Ref. [16] that has been computed at one loop in Ref. [17]. In such cases one must in principle apply the general definition (7) of the coupling constant; nevertheless the form (9) is used quite often in this case (for a kinematical configuration other than T schemes) also as an approximation, especially in relation with the study of Dyson-Schwinger equations.

We conclude this section by recalling that, in any scheme, the standard renormalization flow dictating the evolution with respect to the scale

$$g_R^2(\mu^2) = g_R^2(\mu'^2) \left(\frac{\tilde{Z}_1(\mu'^2)}{\tilde{Z}_1(\mu^2)} \right)^2 F_R^2(\mu^2, \mu'^2) G_R(\mu^2, \mu'^2) \quad (10)$$

will be straightforwardly obtained from the second line of Eq. (7) and the propagators renormalization conditions in Eqs. (2) and (3), where

$$\tilde{Z}_1(\mu^2) = \lim_{\Lambda \rightarrow \infty} \tilde{Z}_1(\mu^2, \Lambda^2) \quad (11)$$

because of the Taylor's nonrenormalization theorem. Of course, Eq. (10) reduces to

$$g_T^2(\mu^2) = g_T^2(\mu'^2) F_R^2(\mu^2, \mu'^2) G_R(\mu^2, \mu'^2) \quad (12)$$

in the T scheme.

1. Pure perturbation theory

In Ref. [18], the three-loop perturbative subtraction of all the three-vertices appearing in the QCD Lagrangian for kinematical configurations with one vanishing momentum has been done [in particular, the one involved in the definition of the coupling by Eq. (9)]. Different definitions of the coupling constant can be related in perturbation theory through relations like

$$\alpha_T(\mu^2) = \bar{\alpha}(\mu^2) \left(1 + \sum_{i=1} c_i \left(\frac{\bar{\alpha}(\mu^2)}{4\pi} \right)^i \right), \quad (13)$$

where $\bar{\alpha}$ is the coupling renormalized according to the usual $\overline{\text{MS}}$ prescription, its standard β function

$$\beta_{\overline{\text{MS}}}(\bar{\alpha}) = \frac{d\bar{\alpha}}{d \ln \mu^2} = -4\pi \sum_{i=0} \bar{\beta}_i \left(\frac{\bar{\alpha}}{4\pi} \right)^{i+2} \quad (14)$$

given at four loops in Ref. [19] ($\bar{\beta}_0$ and $\bar{\beta}_1$ being scheme-independent). On the other hand, since Eq. (9) completely defines the running of the coupling, after properly deriving both its left-hand side and right-hand side, one obtains

$$\begin{aligned} \frac{1}{\alpha_T(\mu^2)} \frac{d\alpha_T(\mu^2)}{d\bar{\alpha}} &= \frac{1}{\beta_{\overline{\text{MS}}}(\bar{\alpha})} \left(2 \lim_{\Lambda \rightarrow \infty} \frac{d}{d \ln \mu^2} \ln F(\mu^2, \Lambda) \right. \\ &\quad \left. + \lim_{\Lambda \rightarrow \infty} \frac{d}{d \ln \mu^2} \ln G(\mu^2, \Lambda) \right) \\ &= \frac{2\tilde{\gamma}(\bar{\alpha}) + \gamma(\bar{\alpha})}{\beta_{\overline{\text{MS}}}(\bar{\alpha})}. \end{aligned} \quad (15)$$

The anomalous dimensions for gluon and ghost propagators,

$$\begin{aligned} \tilde{\gamma}(\bar{\alpha}) &= \lim_{\Lambda \rightarrow \infty} \frac{d \ln \tilde{Z}_{3, \text{MOM}}(\mu^2, \Lambda)}{d \ln \mu^2} = \lim_{\Lambda \rightarrow \infty} \frac{d \ln F(\mu^2, \Lambda)}{d \ln \mu^2} \\ &= - \sum_{i=0} \tilde{\gamma}_i \left(\frac{\bar{\alpha}}{4\pi} \right)^{i+1} \\ \gamma(\bar{\alpha}) &= \lim_{\Lambda \rightarrow \infty} \frac{d \ln Z_{3, \text{MOM}}(\mu^2, \Lambda)}{d \ln \mu^2} = \lim_{\Lambda \rightarrow \infty} \frac{d \ln G(\mu^2, \Lambda)}{d \ln \mu^2} \\ &= - \sum_{i=0} \gamma_i \left(\frac{\bar{\alpha}}{4\pi} \right)^{i+1}, \end{aligned} \quad (16)$$

are both renormalized along MOM prescriptions (i.e., $G_R(\mu^2, \mu^2) = F_R(\mu^2, \mu^2) = 1$) but expanded in terms of $\bar{\alpha}$. Then, Eqs. (13), (14), and (16) can be applied to Eq. (15) and one is led to deal with a coupled system of n algebraic equations to compute the coefficients c_i and determine α_T at n loops. To summarize, the running of coupling constant α_T , although formally defined from a three-point Green function, can be derived from the knowledge of the standard $\overline{\text{MS}}$ β function and only two-points functions for ghost and gluon. These two anomalous dimensions were computed in the $\overline{\text{MS}}$ scheme at four loops in Refs. [20,21] and were converted into the MOM scheme in Ref. [22] for $N_f = 0$ by applying

$$\begin{aligned} \gamma_{\Gamma, \text{MOM}}(\bar{\alpha}) &= \lim_{\Lambda \rightarrow \infty} \frac{d \ln(Z_{\Gamma, \text{MS}}(\mu^2, \Lambda))}{d \ln \mu^2} + \frac{d \ln(\Gamma_{R, \overline{\text{MS}}}(\bar{\alpha}))}{d \ln \mu^2} \\ &\equiv \gamma_{\Gamma, \overline{\text{MS}}}(\bar{\alpha}) + \frac{d\bar{\alpha}}{d \ln \mu^2} \frac{\partial}{\partial \bar{\alpha}} \ln \Gamma_{R, \overline{\text{MS}}}(\bar{\alpha}), \end{aligned} \quad (17)$$

where Γ stands generically for the two bare two-point dressing functions F and G , Γ_R for the renormalized ones² and Z_Γ for the appropriate renormalization constant. Equation (17) provides also the coefficients $\tilde{\gamma}_i$ and γ_i for any N_f (see Appendix A). Thus, one can solve the above-

²The gluon and ghost renormalized propagators in the $\overline{\text{MS}}$ scheme were also provided by Ref. [18].

mentioned coupled system of algebraic equations coming from Eq. (15) with these coefficients and obtain the ones, c_i , in Eq. (13). The first of those coupled equations from Eq. (15) (the one stemming from matching the $1/\alpha$ terms in the two sides) results in the following constraint³:

$$2\tilde{\gamma}_0 + \gamma_0 = \bar{\beta}_0, \quad (18)$$

which, in this context, results from Eq. (9). The three first coefficients c_i in Landau gauge, obtained as above explained [i.e., by substituting the results of Appendix A into Eq. (15)], will be

$$\begin{aligned} c_1 &= \frac{507 - 40N_f}{36}, \\ c_2 &= \frac{76063}{144} - \frac{351}{8}\zeta(3) - \left(\frac{1913}{27} + \frac{4}{3}\zeta(3)\right)N_f + \frac{100}{91}N_f^2 \\ c_3 &= \frac{42074947}{1728} - \frac{60675}{16}\zeta(3) - \frac{70245}{64}\zeta(5) \\ &\quad - \left(\frac{769387}{162} - \frac{8362}{27}\zeta(3) - \frac{2320}{9}\zeta(5)\right)N_f \\ &\quad + \left(\frac{199903}{972} + \frac{28}{9}\zeta(3)\right)N_f^2 - \frac{1000}{729}N_f^3. \end{aligned} \quad (19)$$

These three coefficients obviously define unambiguously the running of α_T given in Eq. (9) up to four loops. In other words, one obtains for the β function of α_T

$$\beta_T(\alpha_T) = \frac{d\alpha_T}{d\ln\mu^2} = -4\pi \sum_{i=0} \tilde{\beta}_i \left(\frac{\alpha_T}{4\pi}\right)^{i+2} \quad (20)$$

the following coefficients up to four loops

$$\begin{aligned} \tilde{\beta}_0 &= \bar{\beta}_0 = 11 - \frac{2}{3}N_f & \tilde{\beta}_1 &= \bar{\beta}_1 = 102 - \frac{38}{3}N_f \\ \tilde{\beta}_2 &= \bar{\beta}_2 - \bar{\beta}_1 c_1 + \bar{\beta}_0(c_2 - c_1^2) \\ &= 3040.48 - 625.387N_f + 19.3833N_f^2 \\ \tilde{\beta}_3 &= \bar{\beta}_3 - 2\bar{\beta}_2 c_1 + \bar{\beta}_1 c_1^2 + \bar{\beta}_0(2c_3 - 6c_2 c_1 + 4c_1^3) \\ &= 100541 - 24423.3N_f + 1625.4N_f^2 - 27.493N_f^3. \end{aligned} \quad (21)$$

These coefficients $\tilde{\beta}_i$ are the same as the ones obtained in Ref. [18] thanks to a direct application of the MOM prescription to the ghost-gluon coupling with vanishing incoming ghost momentum, as it should be. As for the Λ_{QCD} parameters in the two schemes, they are related through

$$\frac{\Lambda_{\overline{\text{MS}}}}{\Lambda_T} = e^{-(c_1/2\beta_0)} = e^{-(507-40N_f/792-48N_f)}. \quad (22)$$

Equation (20) can be integrated and perturbatively inverted

³Equation (18) is a well-known relation verified by scheme-independent coefficients of the ghost and gluon anomalous dimensions and of the β function.

to obtain the following standard four-loop formula for the running coupling,

$$\begin{aligned} \alpha_T(\mu^2) &= \frac{4\pi}{\beta_0 t} \left(1 - \frac{\beta_1}{\beta_0^2} \frac{\log(t)}{t} + \frac{\beta_1^2}{\beta_0^4} \frac{1}{t^2} \left(\left(\log(t) - \frac{1}{2} \right)^2 \right. \right. \\ &\quad \left. \left. + \frac{\tilde{\beta}_2 \beta_0}{\beta_1^2} - \frac{5}{4} \right) \right) + \frac{1}{(\beta_0 t)^4} \left(\frac{\tilde{\beta}_3}{2\beta_0} + \frac{1}{2} \left(\frac{\beta_1}{\beta_0} \right)^3 \right) \\ &\quad \times \left(-2\log^3(t) + 5\log^2(t) + \left(4 - 6 \frac{\tilde{\beta}_2 \beta_0}{\beta_1^2} \right) \right. \\ &\quad \left. \times \log(t) - 1 \right) \quad \text{with} \quad t = \ln \frac{\mu^2}{\Lambda_T^2}. \end{aligned} \quad (23)$$

As a last remark, applying the approximation $\tilde{Z}_1 = 1$ for symmetric (ghost-gluon vertex renormalized at a symmetric momenta configuration) or soft-gluon (vertex renormalized at a vanishing-gluon momenta configuration) schemes implies that the same lattice data for the coupling, obtained through Eq. (9), would be confronted to different perturbative formulae analogous to Eq. (23) with β function coefficients and Λ_{QCD} parameters appropriate for each scheme. Thus, the systematic deviation induced by applying this approximation to the determination of $\Lambda_{\overline{\text{MS}}}$ from the confrontation of perturbation theory and lattice data, provided that β_0 and β_1 are scheme-independent, mainly results from the ratio of Λ_{QCD} to $\Lambda_{\overline{\text{MS}}}$ in Eq. (22). For instance in pure Yang-Mills, if one takes $N_f = 0$ in Eq. (22), it gives a ratio of 0.527 in the T scheme, while the same ratio for instance in symmetric and soft-gluon schemes is 0.463 (14% of error) and 0.429 (23% of error), respectively.

B. OPE power corrections

One of the goals of the present paper consists in obtaining a formula for the QCD running coupling that could be implemented in conjunction with lattice estimates to determine a ‘‘plateau’’ for Λ_{QCD} in terms of the momentum, as will be explained in the next section. In order to extend this plateau to energies as low as possible (of the order of 3 GeV) and to take full advantage of the lattice data in order to reduce the systematic uncertainties, it is mandatory to take into account the gauge-dependent dimension-two operator-product expansion (OPE) power corrections (cf. [7,8,10,23]) to α_T .

The leading power contribution to the ghost propagator

$$(F^{(2)})^{ab}(q^2) = \int d^4x e^{iq \cdot x} \langle T(c^a(x) \bar{c}^b(0)) \rangle \quad (24)$$

can be computed using the [24] OPE, as is done in Ref. [25],

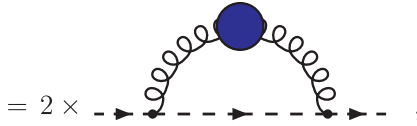
$$T(c^a(x) \bar{c}^b(0)) = \sum_i (c_i)^{ab}(x) O_i(0); \quad (25)$$

here O_i is a local operator, regular when $x \rightarrow 0$, and the

Wilson coefficient c_t contains the short-distance singularity. Equation (25) involves a full hierarchy of terms, ordered according to their mass dimension, among which only $\mathbf{1}$ and $:A_\mu^a A_\nu^b:$ contribute to Eq. (26) in Landau gauge⁴ up to the order $1/q^4$. Then, using Eq. (25) into Eq. (24), we obtain

$$\begin{aligned} (F^{(2)})^{ab}(q^2) &= (c_0)^{ab}(q^2) + (c_2)_{st}^{ab\sigma\tau}(q^2) \langle :A_\sigma^s(0) A_\tau^t(0): \rangle \\ &+ \dots \\ &= (F_{\text{pert}}^{(2)})^{ab}(q^2) + w^{ab} \frac{\langle A^2 \rangle}{4(N_C^2 - 1)} + \dots \end{aligned} \quad (26)$$

where

$$w^{ab} = (c_2)_{st}^{ab\sigma\tau} \delta^{st} g_{\sigma\tau} = \frac{1}{2} \delta^{st} g_{\sigma\tau} \frac{\int d^4x e^{iq \cdot x} \langle \tilde{A}_\tau^{t'}(0) T \left(c^a \bar{c}^b \right) \tilde{A}_\sigma^{s'}(0) \rangle_{\text{connected}}}{G_{\sigma\sigma'}^{(2)} G_{\tau\tau'}^{(2)}}$$


$$= 2 \times \text{Sunset Diagram}, \quad (27)$$

and the Shiffman-Vainshtein-Zakharov (SVZ) factorization [26] is invoked to compute the Wilson coefficients. Thus, one should compute the ‘‘sunset’’ diagram of the last line of Eq. (27), that binds the ghost propagator to the gluon condensate (where the blue bubble means contracting the color and Lorentz indices of the incoming legs with $1/2\delta_{st}\delta_{\sigma\tau}$) to obtain the leading nonperturbative contribution (of course, the first Wilson coefficient gives trivially the perturbative propagator).

Finally,

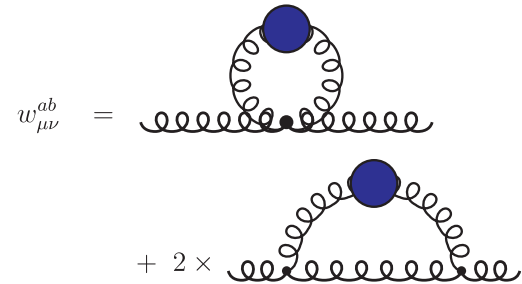
$$\begin{aligned} (F_R^{(2)})^{ab}(q^2, \mu^2) &= (F_{R,\text{pert}}^{(2)})^{ab}(q^2, \mu^2) \left(1 + \frac{3}{q^2} \frac{g_R^2 \langle A^2 \rangle_{R,\mu^2}}{4(N_C^2 - 1)} \right) \\ &+ \mathcal{O}(g^4, q^{-4}), \end{aligned} \quad (28)$$

where the A^2 condensate is renormalized at the subtraction point $q^2 = \mu^2$, according to the MOM scheme definition, by imposing the tree-level value to the Wilson coefficient at the renormalization point. As far as we do not need to deal with the anomalous dimension of the A^2 operator, we can factorize the tree-level ghost propagator. The ghost dressing function is then written as

$$F_R(q^2, \mu^2) = F_{R,\text{pert}}(q^2, \mu^2) \left(1 + \frac{3}{q^2} \frac{g_R^2 \langle A^2 \rangle_{R,\mu^2}}{4(N_C^2 - 1)} \right), \quad (29)$$

where the multiplicative correction to the purely perturbative $F_{R,\text{pert}}$ is determined up to corrections of the order $1/q^4$ or $\ln q/\mu$ (the Wilson coefficient at the leading logarithm is computed in Appendix B).

We can handle in the same way (see Refs. [7,8]) the OPE power correction to the gluon propagator and obtain



$$\begin{aligned} w_{\mu\nu}^{ab} &= \text{Sunset Diagram} \\ &+ 2 \times \text{Sunset Diagram} \\ &= \frac{3g^2}{q^2} (G_{\text{pert}}^{(2)})_{\mu\nu}^{ab}. \end{aligned} \quad (30)$$

Then, after renormalization, one gets

$$\begin{aligned} (G_R^{(2)})_{\mu\nu}^{ab}(q^2, \mu^2) &= (G_{R,\text{pert}}^{(2)})_{\mu\nu}^{ab}(q^2, \mu^2) + (w_{\mu\nu}^{ab})_{R,\mu^2} \\ &\times \frac{\langle A^2 \rangle_{R,\mu^2}}{4(N_C^2 - 1)} + \dots \\ &= (G_{R,\text{pert}}^{(2)})_{\mu\nu}^{ab}(q^2, \mu^2) \left(1 + \frac{3}{q^2} \right. \\ &\left. \times \frac{g_R^2 \langle A^2 \rangle_{R,\mu^2}}{4(N_C^2 - 1)} \right) + \mathcal{O}(g^4, q^{-4}). \end{aligned} \quad (31)$$

And an appropriate projection gives for the gluon dressing function

$$G_R(q^2, \mu^2) = G_{R,\text{pert}}(q^2, \mu^2) \left(1 + \frac{3}{q^2} \frac{g_R^2 \langle A^2 \rangle_{R,\mu^2}}{4(N_C^2 - 1)} \right). \quad (32)$$

Finally, putting together the defining relation Eq. (9) and the results Eqs. (29) and (32) we get

⁴The operators with an odd number of fields ($d = 1, 3/2; \partial_\mu A$, and $\partial_\mu \bar{c}$) cannot satisfy color and Lorentz invariance and do not contribute a nonzero nonperturbative expectation value, and \bar{c} does not contribute either because of the particular tensorial structure of the ghost-gluon vertex.

$$\begin{aligned}
\alpha_T(\mu^2) &= \lim_{\Lambda \rightarrow \infty} \frac{g_0^2}{4\pi} F^2(\mu^2, \Lambda) G(\mu^2, \Lambda) \\
&= \lim_{\Lambda \rightarrow \infty} \frac{g_0^2}{4\pi} \overbrace{F^2(q_0^2, \Lambda) G(q_0^2, \Lambda) F_R^2(\mu^2, q_0^2) G_R(\mu^2, q_0^2)}^{\alpha_T^{\text{pert}}(q_0^2)} \\
&= \underbrace{\alpha_T^{\text{pert}}(q_0^2) F_{R,\text{pert}}^2(\mu^2, q_0^2) G_{R,\text{pert}}(\mu^2, q_0^2)}_{\alpha_T^{\text{pert}}(\mu^2)} \\
&\quad \times \left(1 + \frac{9}{\mu^2} \frac{g_T^2(q_0^2) \langle A^2 \rangle_{R, q_0^2}}{4(N_C^2 - 1)} \right), \quad (33)
\end{aligned}$$

where $q_0^2 \gg \Lambda_{\text{QCD}}$ is some perturbative scale and the β function, and its coefficients in Eq. (21) of course describe the running of the perturbative part of the evolution α_T^{pert} .

The Wilson coefficient at the leading logarithm for the T scheme MOM running coupling is presented in Appendix B, where we also show that the inclusion of the logarithmic correction would induce no significant effect, provided that the coupling multiplying A^2 inside the bracket is taken to be renormalized also in T scheme. Thus, for the sake of simplicity, Eq. (33) will be applied for our analysis in the next section.

III. DATA ANALYSIS

In the following, we will first propose a plateau-procedure exploiting Eq. (33) to get a reliable estimate of the Λ_{QCD} parameter from the lattice and we will apply it to previously published quenched lattice data [22,25] as a check of the method.

A. The plateau method

The goal being to get a trustworthy estimate of the $\Lambda_{\overline{\text{MS}}}$ parameter, one could attempt to do it by inverting the perturbative formula Eq. (23) and using in the *inverted* formula the lattice estimates of the running coupling obtained by means of Eq. (9) for as many lattice momenta as possible. Then, one should look for a plateau of $\Lambda_{\overline{\text{MS}}}$ in terms of momenta in the high-energy perturbative regime (this was done with the coupling defined by the three-gluon vertex in [4,5]). In the next subsection, Fig. 2(a) shows the estimates of $\Lambda_{\overline{\text{MS}}}$ so calculated for the lattice data presented in Refs. [22,25] over $9 \lesssim p^2 \lesssim 33 \text{ GeV}^2$.

However, in order to take advantage of the largest possible momenta window one can use instead Eq. (33). In this way we shall hopefully be able to extend towards *low* momenta the region over which to look for the best possible values of the gluon condensate and of $\Lambda_{\overline{\text{MS}}}$.⁵ In other words, one requires the best-fit to a constant of

⁵This increases the statistics and reduces errors. It also avoids some possible systematic deviation appearing when lattice momentum components, in lattice units, approach $\pi/2$ (Brillouin's region border).

$$(x_i, y_i) \equiv (p_i^2, \Lambda(\alpha_i)), \quad \text{with: } \alpha_i = \frac{\alpha_{\text{Latt}}(p_i^2)}{1 + \frac{c}{p_i^2}}, \quad (34)$$

where $\Lambda(\alpha)$ is obtained by inverting the perturbative four-loop formula Eq. (23) and c results from the best fit [it appeared written in terms of the gluon condensate in Eq. (33)]. Thus, $\Lambda(\alpha)$ reaches a plateau (if it does) behaving in terms of the momentum as a constant that we will take as our estimate of $\Lambda_{\overline{\text{MS}}}$. Of course, this is nothing but a fitting strategy for a 2-parameters ($\Lambda_{\overline{\text{MS}}}$ and $\langle A^2 \rangle$) fit of the estimates of Eq. (9) from lattice data.

B. Applying the method

The lattice data that we will exploit here to check the method we have explained above were previously presented in Ref. [22]. We refer to this work for all the details concerning the lattice implementation: algorithms, action, Faddeev-Popov operator inversion, etc.

The parameters of the whole set of simulations are described in Table I.

1. The scaling from different lattices

It should first be noted that the scaling of Eq. (9) from the several lattices we use is indeed satisfactory. The prescription of taking the infinite cutoff limit in Eq. (9) means in practice to have the lattice artifacts under control. This is in fact the case for UV ones. In particular, the hypercubic artifacts behaving as $\mathcal{O}(a^k \sum p_i^k)$ for the lattice propagators we analyze were cured, as explained in [22], by exploiting the H_4 symmetry.

As an indirect way of testing that scaling, we consider all the lattice propagators as functions of the momentum *measured in lattice units*, [i.e. with dimensionless momenta $p_{\text{Lat}} = a(\beta)p$, where $a(\beta)$ is the lattice spacing in physical units at the particular bare lattice coupling $g_0^2 = 6/\beta$], and determine the ratios of $a(\beta)$'s for the scaling to work. Then, still working in lattice units, the best-fit parameters to be obtained by applying the plateau-method will be $a(\beta)\Lambda_{\overline{\text{MS}}}$ and $a^2(\beta)g_T^2 \langle A^2 \rangle_R$, and the ratio of those best-fit parameters for different lattices will provide the ratio of the corresponding lattice spacings.

In Table II, the ratio of lattice spacings obtained by the standard string-tension method [1] is compared with those obtained as explained above. More precisely: (i) we first determine $\Lambda_{\overline{\text{MS}}} a(6.2)$ and $a^2(6.2)g_T^2 \langle A^2 \rangle_R$ for the lattice data with $\beta = 6.2$; (ii) then, for each new β , we determine

TABLE I. Run parameters of the exploited data [22].

β	Volume	a^{-1} (GeV)	Number of gauge configurations
6.0	16^4	1.96	1000
6.0	24^4	1.96	500
6.2	24^4	2.75	500
6.4	32^4	3.66	250

TABLE II. Comparison of lattice spacing ratios obtained by means of the scaling of Eq. (9) as explained in the text and of the string-tension method.

β	Volume	$a(\beta)/a(6.2)$ (this work)	$a(\beta)/a(6.2)$ [1]	Deviations (%)
6.0	16^4	1.368	1.378	0.7
6.0	24^4	1.322	1.378	4.1
6.2	24^4	1	1	0
6.4	32^4	0.768	0.751	2.2

$x = a(\beta)/a(6.2)$ in such a way that a plateau for $xa(6.2)\Lambda_{\overline{\text{MS}}}$ is obtained with a gluon condensate given by $x^2 a^2(6.2)g_T^2 \langle A^2 \rangle_R$. They agree very well, at least for the ratios computed for the three lattice simulations with roughly the same physical volume: $\beta = 6.0(L = 16 = 1.58 \text{ fm})$, $\beta = 6.2(L = 24 = 1.72 \text{ fm})$, $\beta = 6.4(L = 32 = 1.72 \text{ fm})$. A slightly larger discrepancy ($\sim 4\%$) appears when comparing with data for the largest lattice ($\beta = 6.0, L = 24 = 2.37 \text{ fm}$). We suspect that this is the manifestation of a finite-volume effect. Actually, if we compare the two simulations at $\beta = 6.0$ for different volumes (see Fig. 1), such an effect can be seen, although it decreases as the physical momentum increases (and becomes in practice negligible at $p^2 \sim 9 \text{ GeV}^2$).

Thus, one can conclude that the scaling of the coupling defined by Eq. (9) for $p^2 \gtrsim 9 \text{ GeV}^2$ is very good. Conversely, this argument provides an alternative method to determine the lattice size for a simulation at a given β in terms of the one known in physical units at any other one.

2. Looking for the plateau

In Fig. 2(a), we show the estimates of $\Lambda_{\overline{\text{MS}}}$ obtained when interpreting the lattice coupling computed by Eq. (9) for any momentum $9 \leq p^2 \leq 33 \text{ GeV}^2$ in terms of the *inverted* four-loop perturbative formula for the coupling, Eq. (23). The estimates systematically decrease as the squared momentum increases until around 22 GeV^2 ; above this value, only a noisy pattern results. In Fig. 2(b), the same is plotted but inverting instead the nonperturbative formula including power corrections, Eq. (33). The value of the gluon condensate has been determined by requiring a

plateau to exist (as explained in the previous section) over the total momenta window.

One should realize that, had we not taken into account the noisy ballpark of points above 22 GeV^2 and had we considered the perturbative regime as reached at that momentum, we would have gotten an estimate of $\Lambda_{\overline{\text{MS}}}$ roughly $35\text{--}40 \text{ MeV}$ above the one obtained from the nonperturbative formula. In other words, the nonperturbative analysis seems to indicate that the perturbative regime is far from being achieved at $p = 5 \text{ GeV}$. This is illustrated in Fig. 3 in which, adopting for $\Lambda_{\overline{\text{MS}}}$ the value 224 MeV which results from the nonperturbative analysis, we plot against the square of the renormalization momentum the coupling constant as computed by means of the nonperturbative formula (33) (upper red curve) and of the perturbative one (23) (lower blue curve). Displayed are also the lattice data, i.e. the values of α_T obtained from Eq. (9). In Fig. 3(a) one sees that the nonperturbative approach provides a fairly good agreement with the data, the χ^2 being 1.3 per degree of freedom. On the contrary there is a clear disagreement with the perturbative formula. Furthermore, one can extrapolate the value of α_T up to very high momenta with Eq. (33), $p^2 \sim 300\text{--}500 \text{ GeV}^2$, where the purely perturbative Eq. (23) and the nonperturbative Eq. (33), both with the same $\Lambda_{\overline{\text{MS}}}$, generate in practice the same results. The plot of Fig. 3(b) shows indeed that the curve for the coupling extrapolated in this way joins perfectly the lattice estimates at high momenta taken from [9]. Thus, the inclusion of the nonperturbative OPE power correction Eq. (33), to describe the running of the coupling eliminates effectively the observed systematic deviations for the estimates of $\Lambda_{\overline{\text{MS}}}$ from the momenta window from 3 to 5 GeV [Fig. 2

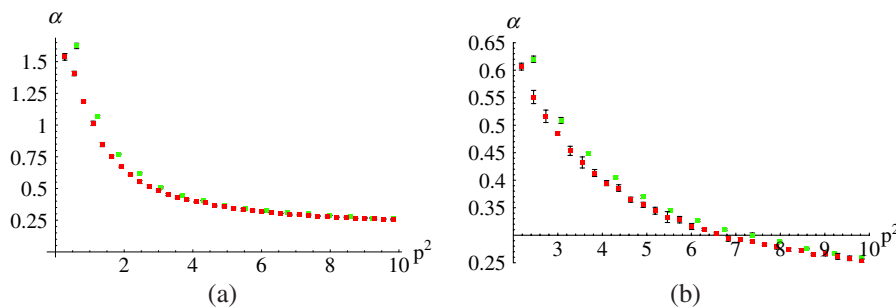


FIG. 1 (color online). (a) Plot of α_T defined by Eq. (9) in terms of the square of the renormalization momentum as computed from the two lattices at $\beta = 6.0$ with different volumes: $V = 16^4$ (gray [green] boxes) and $V = 24^4$ (black [red] boxes). (b) A zoom onto the high momenta region of the left plot.

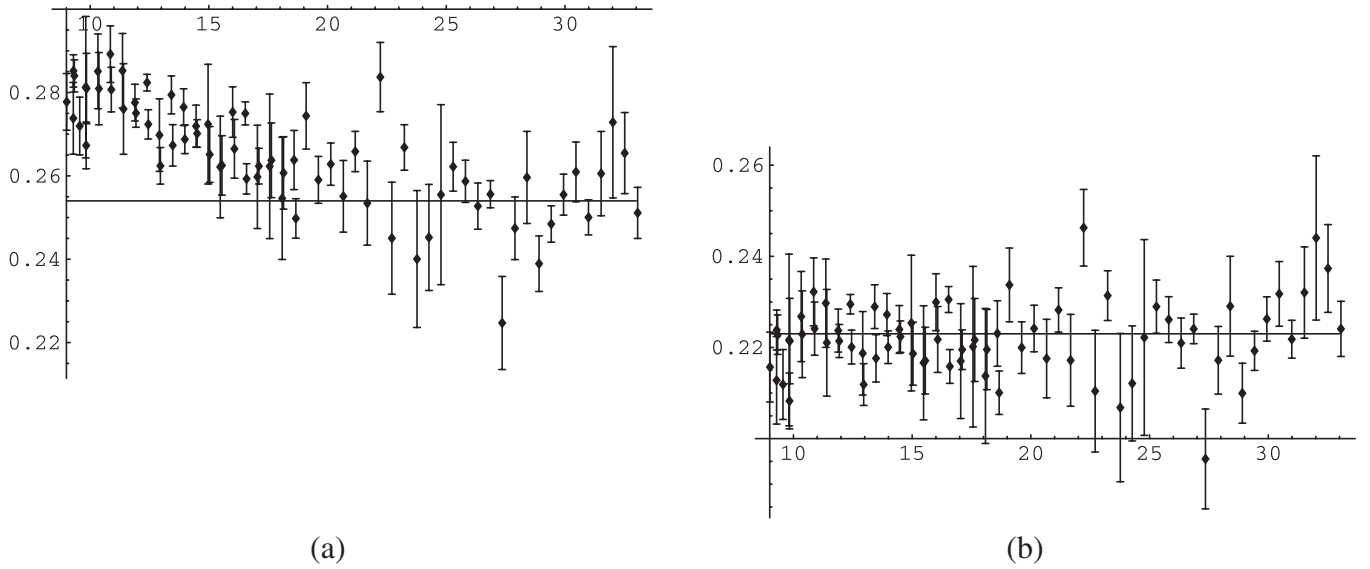


FIG. 2. (a) Plot of $\Lambda_{\overline{\text{MS}}}$ (in GeV) computed by the inversion of the four-loop perturbative formula Eq. (23) as a function of the square of the momentum (in GeV^2); the coupling is estimated from the lattice data through Eq. (9). (b) Same as plot (a) except for applying the nonperturbative formula Eq. (33) for the coupling and looking for the gluon condensate generating the best plateau over $9 \lesssim p^2 \lesssim 33 \text{ GeV}^2$.

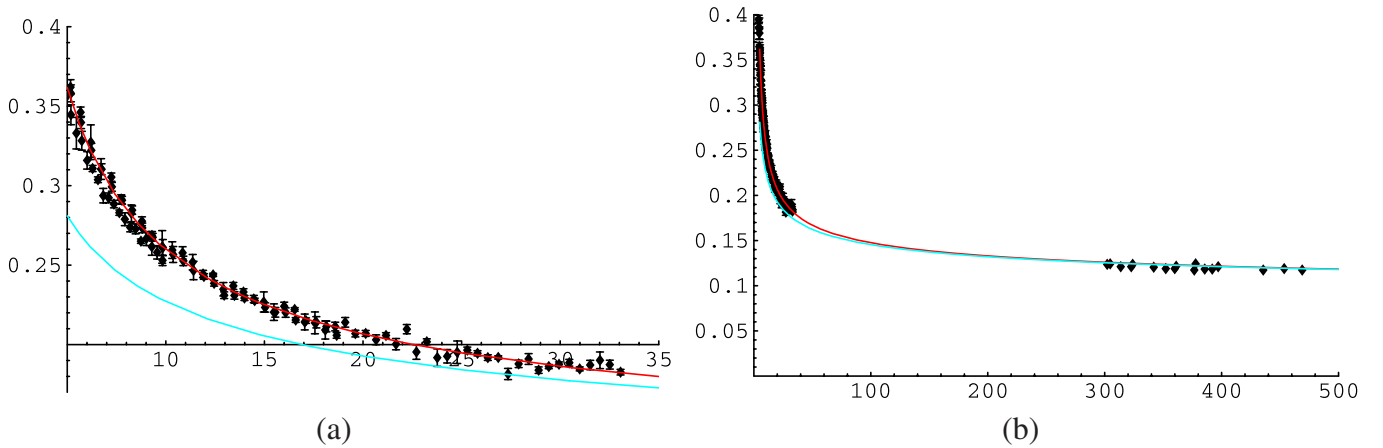


FIG. 3 (color online). (a) Plot of α_T defined by Eq. (9) in terms of the square of the renormalization momentum: the upper (red) line is computed with Eq. (33) with $\Lambda_{\overline{\text{MS}}} = 224 \text{ MeV}$, the lower (blue) one with Eq. (23) for the same $\Lambda_{\overline{\text{MS}}}$ and the data are obtained from the lattice data set up in Table I. (b) The same but with some additional lattice estimates for the coupling at very high momenta ($300\text{--}500 \text{ GeV}^2$) taken from [9].

(a)] and essentially leads to the same estimate as was found from the perturbative regime at very high momentum.

Thus, we have been able to obtain simultaneous best-fit values for both the gluon condensate and $\Lambda_{\overline{\text{MS}}}$. It is however manifest that they are correlated by their determination: the larger the gluon condensate is, the smaller the value of $\Lambda_{\overline{\text{MS}}}$ has to be. In Fig. 4, we plot the ellipsoid defined by⁶ $\chi^2(\Lambda_{\overline{\text{MS}}}, g_T^2 \langle A^2 \rangle_R) = \chi_{\min}^2 + 1$ for a fitting

⁶The errors on the lattice estimates of the coupling that were used to compute χ^2 were obtained by propagating the ones computed through the jackknife method for F and G in [22].

window defined by $p^2 > 9 \text{ GeV}^2$ and for one restricted to $p^2 > 14 \text{ GeV}^2$. It is seen that, neglecting other sources of errors like, for instance, the calibration of the lattices, but being conservative with the choice of the fitting window, one can conclude that our best-fit parameters incorporating only⁷ statistical errors are

$$\Lambda_{\overline{\text{MS}}}^{N_f=0} = 224_{-5}^{+8} \text{ MeV} \quad g_T^2 \langle A^2 \rangle_R = 5.1_{-1.1}^{+0.7} \text{ GeV}^2. \quad (35)$$

⁷We define the errors by taking the larger ellipsoid and this could be considered to account for some systematic effect related to the choice of the fitting window.

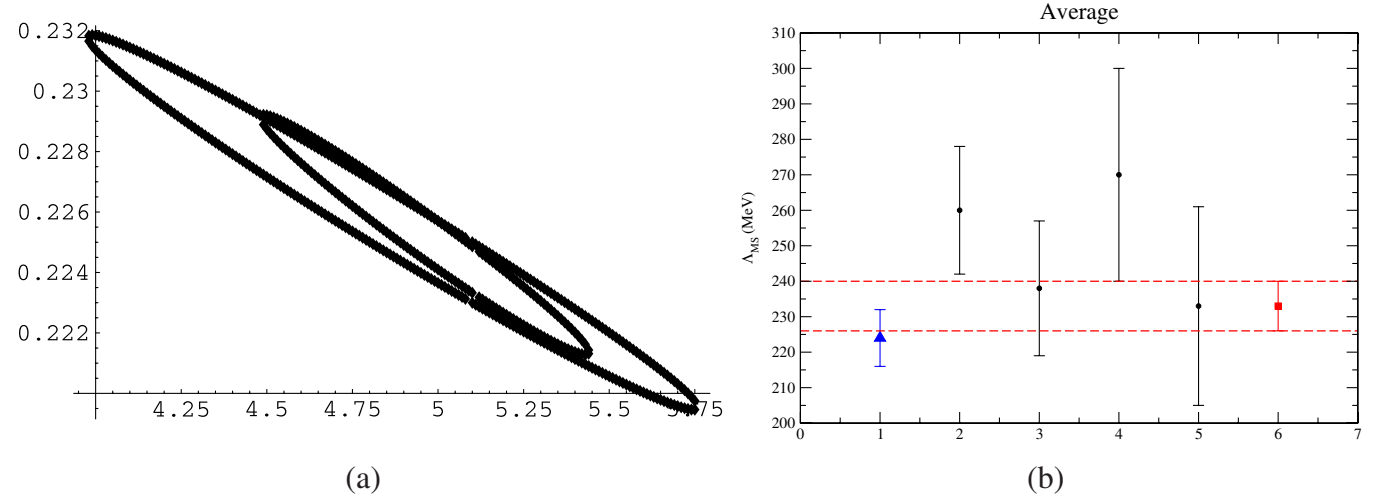


FIG. 4 (color online). (a) The ellipsoid defined by $\chi^2(\Lambda_{\overline{\text{MS}}}, g_T^2 \langle A^2 \rangle_R) = \chi_{\min}^2 + 1$. The y axis is for $\Lambda_{\overline{\text{MS}}}$ expressed in GeV and x axis for $g_T^2 \langle A^2 \rangle_R$ in GeV^2 . The small ellipsoid is obtained for a fitting window defined by $p^2 > 9 \text{ GeV}^2$ and the larger is for $p^2 > 14 \text{ GeV}^2$. (b) Comparison with previous estimates of $\Lambda_{\overline{\text{MS}}}$ in pure Yang-Mills collected in Table III; the blue triangle stands for the estimate in this work and the red square for the *average* of the five estimates presented in the plot. The $1-\sigma$ error interval for the average (dashed red line) was estimated by treating the errors in Table III as purely statistical ones.

TABLE III. Comparison of estimates of $\Lambda_{\overline{\text{MS}}}$ obtained from the analysis of the ghost-gluon vertex in this work (first column), the asymmetric 3-gluon vertex (second column), the symmetric 3-gluon vertex (third column), the ratio of gluon and ghost dressing functions (fourth column) and with the Schrödinger functional method (last column). The gluon condensate $\langle A^2 \rangle_{R,\mu}$ has been obtained at the renormalization momentum $\mu = 10 \text{ GeV}$, for the sake of comparison with the other estimates, from Eq. (35) by applying $g^2(\mu^2 = 100 \text{ GeV}^2)/4\pi = 0.15$.

	F^2G (this work)	Asymmetric 3-gluon [8]	Symmetric 3-gluon [8]	F/G [25]	Schrödinger [2]
$\Lambda_{\overline{\text{MS}}} \text{ (MeV)}$	244^{+8}_{-5}	260(18)	233(28)	270(30)	238(19)
$\sqrt{\langle A^2 \rangle_{R,\mu}} \text{ (GeV)}$	1.64(17)	2.3(6)	1.9(3)	1.3(4)	—

These values are in very good agreement with the previous estimates from quenched lattice simulations of the three-gluon Green function [7,8] or, in the case of $\Lambda_{\overline{\text{MS}}}$, from the implementation of the Schrödinger functional method [2], although slightly larger than the one obtained by the ratio of ghost and gluon dressing functions [25] [see Fig. 4(b) and Table III]. Concerning the gluon condensate estimate only, it is worth pointing out that it can be computed at the renormalization momentum⁸ $\mu^2 = 100 \text{ GeV}^2$ (see Table III) and it also agrees very well with the estimate from the analysis of the quark propagator vector part Z_ψ that gives $\sqrt{\langle A^2 \rangle_{R,\mu=10 \text{ GeV}}} = 1.76(8) \text{ GeV}$

⁸Neglecting the leading logarithm for the Wilson coefficient implies that $g^2 \langle A^2 \rangle$, one of the quantities determined through our fits in this paper, is a renormalization-group invariant and does not depend on the renormalization momentum, but $\langle A^2 \rangle$ does. We fix anyhow $\mu^2 = 100 \text{ GeV}^2$ and compute $\langle A^2 \rangle$ at that momentum, for the sake of comparison with other determinations of the gluon condensate in literature.

[27]. A comment about higher-order nonperturbative OPE corrections is in order at this point. The neglect of their contribution (at least of the order of $\mathcal{O}(1/p^4)$) could explain the deviation of the lattice estimates from our OPE formula Eq. (33) below $p^2 = 9 \text{ GeV}$. However, the consistency with other calculations shown above and the very good agreement of our formula with lattice data at very high momenta (see Fig. 3) guarantee that the impact of those high-order OPE corrections, as a possible source of uncertainty in determining $\Lambda_{\overline{\text{MS}}}$ and the gluon condensate over our fitting window, is indeed negligible.

As a final remark, had we taken into account the leading-logarithm behavior of the Wilson coefficient for the running coupling [applied Eq. (B7) instead of Eq. (33)], the parameters so fitted would not significantly differ from those in Eq. (35): We estimate a difference of $\sim 4\%$ in the determination of $g_T^2 \langle A^2 \rangle_R$ and less than 0.5% in that of $\Lambda_{\overline{\text{MS}}}$.

IV. CONCLUSIONS

In the present paper we reconsider in some detail the determination of $\Lambda_{\overline{\text{MS}}}$ from gluon and ghost Green functions using the MOM scheme. We stick here to the quenched case, or rather to the pure Yang-Mills $SU(3)$ theory, having of course in mind to apply what we learn also to the unquenched situation.

A. Ghost-gluon vertex

We give some details about the proper renormalization of the ghost-gluon vertex in the MOM scheme mainly because we realized that there is some carelessness in the literature. An obvious remark is that applying MOM to a vertex function needs to specify the kinematics of the renormalization point. Renormalizing at the scale μ may be performed in the symmetric case, with the three momenta at the renormalization scale ($p^2 = \mu^2$) or in the soft-gluon limit ($p_{\text{gluon}} = 0$, $p_{\text{ghost}}^2 = \mu^2$), or with a vanishing incoming ghost momentum, etc. The latter case is the one in which Taylor's theorem applies which leads to $\tilde{Z}_1 = 1$. We present in Sec. II A an alternative derivation of the perturbative renormalization of the coupling constant in the latter scheme, defined by Eq. (9), in agreement with the result by Chetyrkin [18]. The other kinematics lead to a finite but nontrivial $\tilde{Z}_1 = 1 + O(\alpha^2)$. This difference has been often overlooked, presumably because it is assumed to be small. However, as we have shown in Sec. II A, applying $\tilde{Z}_1 = 1$ to the symmetric case leads to a 14% systematic error on $\Lambda_{\overline{\text{MS}}}$ while it gives 23% when applied to the soft-gluon limit.

B. The $\Lambda_{\overline{\text{MS}}}$ plateau

$\Lambda_{\overline{\text{MS}}}$ is a constant independent of the scale μ . Inverting the perturbative expansion of the coupling constant one can invert Eq. (23) leading for each μ to $\Lambda_{\overline{\text{MS}}}(\mu^2)$ from $\alpha_T(\mu^2)$.⁹ If we were in a perturbative region of μ $\Lambda_{\overline{\text{MS}}}(\mu^2)$ should not depend on μ up to statistical errors. One should see a nice plateau. Figure 2(a) shows that this is far from being the case up to $\mu^2 = 30 \text{ GeV}^2$. We have since long advocated that there is a sizeable nonperturbative contribution from the vacuum expectation value of the unique (in Landau gauge) dimension-two operator $\langle A^2 \rangle$. We propose to fit this condensate by adjusting the resulting $\Lambda_{\overline{\text{MS}}}$ to a plateau. This is successfully achieved (see Fig. 2 (b)). Since we scan a large window in the scale μ we believe that we are in a position to claim that we indeed see a nonperturbative $O(1/\mu^2)$ contribution rather than the effect of logarithmically behaved higher orders in perturbation theory ($O(\alpha^5)$).

⁹This can be done in any MOM scheme using the appropriate equivalent to Eq. (23).

C. Comparison of different estimates of $\Lambda_{\overline{\text{MS}}}$

We have performed a comparison of different estimates of $\Lambda_{\overline{\text{MS}}}$ and $\langle A^2 \rangle$ in the pure Yang-Mills theory using the coupling constant defined in Eq. (9), the MOM coupling constant from symmetric three-gluon vertex function, the MOM coupling constant from the three-gluon vertex function with one vanishing momentum and from the ghost to gluon propagator ratio, and also with the estimate of $\Lambda_{\overline{\text{MS}}}$ from the Schrödinger functional approach. The result is reported in Table III and Fig. 4(b). The agreement is quite satisfactory. Figure 3(b) shows also a good agreement of our fit from $\alpha_T(\mu^2)$ with very large μ measurements from [9]. Notice also that $\Lambda_{\overline{\text{MS}}}$ from $\alpha_T(\mu^2)$ has the smallest statistical errors due to the fact that it relies only on a propagator, not on noisier three-point Green functions.

This opens a possibility of using the matching of $\Lambda_{\overline{\text{MS}}}$ as computed from different lattices in order to fit the lattice spacing ratio. One might also match directly $\alpha_T(\mu^2)$ from different lattices, a procedure which is not constrained to large scales and does not need to estimate the $\langle A^2 \rangle$ condensate. In fact from Eq. (9) we get directly a quantity which should be independent of the lattice spacing at the same μ in physical units, up to $O(1/a^2)$ artifacts. This method is complementary to the use of Sommer's parameter r_0 [28] and it also only depends on gauge fields.

APPENDIX A: GHOST AND GLUON PROPAGATORS ANOMALOUS DIMENSION IN MOM

The ghost and gluon anomalous dimension can be computed in the MOM scheme by applying Eq. (17) with the results obtained in $\overline{\text{MS}}$ for the radiative corrections of all the relevant Green functions [18,20,21]. Thus, one obtains for the coefficients defined in Eq. (16)

$$\begin{aligned} \tilde{\gamma}_0 &= \frac{9}{4} \tilde{\gamma}_1 = \frac{813}{16} - \frac{13N_f}{4} \\ \tilde{\gamma}_2 &= \frac{157303}{64} - \frac{14909N_f}{48} + \frac{125N_f^2}{18} - \frac{5697\zeta(3)}{32} \\ &\quad - \frac{21}{4} N_f \zeta(3) \\ \tilde{\gamma}_3 &= \frac{219384137}{1536} - \frac{30925009N_f}{1152} + \frac{288155N_f^2}{216} \\ &\quad - \frac{2705N_f^3}{162} - \frac{9207729\zeta(3)}{512} + \frac{132749}{96} N_f \zeta(3) \\ &\quad - \frac{19}{2} N_f^2 \zeta(3) - \frac{221535\zeta(5)}{32} + \frac{15175}{16} N_f \zeta(5), \quad (\text{A1}) \end{aligned}$$

$$\begin{aligned}
\gamma_0 &= \frac{13}{2} - \frac{2N_f}{3} & \gamma_1 &= \frac{3727}{24} - \frac{250N_f}{9} + \frac{20N_f^2}{27} \\
\gamma_2 &= \frac{2127823}{288} - \frac{9747\zeta(3)}{16} + N_f \left(-\frac{5210}{3} + \frac{119\zeta(3)}{3} \right) \\
&\quad + N_f^2 \left(\frac{1681}{18} + \frac{16\zeta(3)}{9} \right) - \frac{200N_f^3}{243} \\
\gamma_3 &= \frac{3011547563}{6912} - \frac{18987543\zeta(3)}{256} - \frac{1431945\zeta(5)}{64} \\
&\quad + N_f \left(-\frac{221198219}{1728} + \frac{2897113\zeta(3)}{216} + \frac{845275\zeta(5)}{96} \right) \\
&\quad + N_f^2 \left(\frac{6816713}{648} - \frac{60427\zeta(3)}{162} - \frac{4640\zeta(5)}{9} \right) \\
&\quad + N_f^3 \left(-\frac{373823}{1458} - \frac{88\zeta(3)}{27} \right) + \frac{2000N_f^4}{2187}. \tag{A2}
\end{aligned}$$

These coefficients appear for the expansion, given by Eq. (17), of the MOM-renormalized ghost and gluon anomalous dimension in terms of the $\overline{\text{MS}}$ coupling. However, provided that the β function for any other renormalization scheme is known, it can be applied to replace $\alpha_{\overline{\text{MS}}}$ in Eq. (16) by the coupling in that scheme.

APPENDIX B: WILSON COEFFICIENTS AT LEADING LOGARITHMS

The purpose of this appendix is to present up to leading logarithms the subleading Wilson coefficients in Eqs. (29) and (32) and, in view of checking the validity of neglecting those logarithms, estimate their impact on the momenta window we use for our fits. Following [8], let us write

$$\begin{aligned}
G_R(q^2, \mu^2) &= c_0 \left(\frac{q^2}{\mu^2}, \alpha(\mu^2) \right) + c_2 \left(\frac{q^2}{\mu^2}, \alpha(\mu^2) \right) \\
&\quad \times \frac{\langle A_R^2 \rangle_\mu}{4(N_c^2 - 1)q^2} \\
F_R(q^2, \mu^2) &= \tilde{c}_0 \left(\frac{q^2}{\mu^2}, \alpha(\mu^2) \right) + \tilde{c}_2 \left(\frac{q^2}{\mu^2}, \alpha(\mu^2) \right) \\
&\quad \times \frac{\langle A_R^2 \rangle_\mu}{4(N_c^2 - 1)q^2} \tag{B1}
\end{aligned}$$

for gluon and ghost propagators. Then, with the help of the appropriate renormalization constants one can rewrite Eq. (B1) in terms of bare quantities

$$\begin{aligned}
G(q^2, \Lambda^2) &= Z_3(\mu^2, \Lambda^2) c_0 \left(\frac{q^2}{\mu^2}, \alpha(\mu^2) \right) \\
&\quad + Z_3(\mu^2, \Lambda^2) Z_{A^2}^{-1}(\mu^2, \Lambda^2) c_2 \left(\frac{q^2}{\mu^2}, \alpha(\mu^2) \right) \\
&\quad \times \frac{\langle A^2 \rangle}{4(N_c^2 - 1)q^2}, \tag{B2}
\end{aligned}$$

where $A_R^2 = Z_{A^2}^{-1} A^2$. For the ghost dressing function

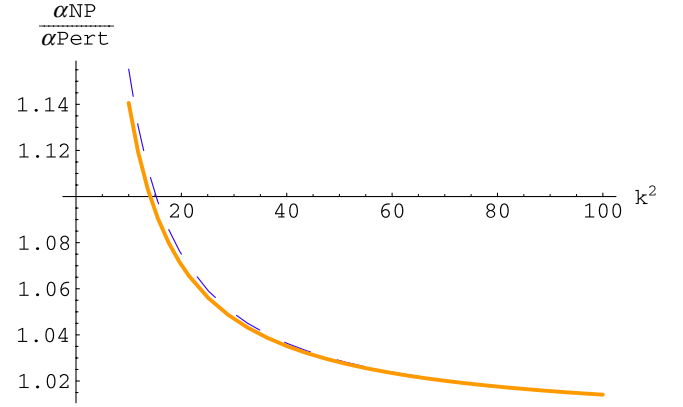


FIG. 5 (color online). $\alpha^{\text{NP}}/\alpha^{\text{pert}}$ in terms of the square of the momentum computed by using both Eq. (B7) (dashed blue) and Eq. (33) (solid red).

$F(q^2, \Lambda^2)$, equations totally analogous to Eqs. (B1) and (B2), with \tilde{c}_i and \tilde{Z}_3 in place of c_i and Z_3 can be obtained. Now, as the μ dependence of both the left-hand side and right-hand side of Eq. (B2) should match each other for any q , one can take the logarithmic derivative with respect to μ and infinite cutoff limit, term by term, on right-hand side and obtain

$$\begin{aligned}
\gamma(\alpha(\mu^2)) + \left\{ \frac{\partial}{\partial \log \mu^2} + \beta(\alpha(\mu^2)) \frac{\partial}{\partial \alpha} \right\} \text{Inc}_0 \left(\frac{q^2}{\mu^2}, \alpha(\mu^2) \right) &= 0 \\
-\gamma_{A^2}(\alpha(\mu^2)) + \gamma(\alpha(\mu^2)) + \left\{ \frac{\partial}{\partial \log \mu^2} + \beta(\alpha(\mu^2)) \frac{\partial}{\partial \alpha} \right\} \\
\times \text{Inc}_2 \left(\frac{q^2}{\mu^2}, \alpha(\mu^2) \right) &= 0, \tag{B3}
\end{aligned}$$

where $\gamma(\alpha(\mu^2))$ is the gluon propagator anomalous dimension defined in Eq. (16) and

$$\begin{aligned}
\gamma_{A^2}(\alpha(\mu^2)) &= \lim_{\Lambda \rightarrow \infty} \frac{d}{d \ln \mu^2} \ln Z_{A^2}(\mu^2, \Lambda^2) \\
&= -\gamma_0^{A^2} \frac{\alpha(\mu^2)}{4\pi} + \dots \tag{B4}
\end{aligned}$$

Both Eqs. (B3) can be finally combined to give

$$\left\{ -\gamma_{A^2}(\alpha(\mu^2)) + \frac{\partial}{\partial \log \mu^2} + \beta(\alpha(\mu^2)) \frac{\partial}{\partial \alpha} \right\} \frac{c_2 \left(\frac{q^2}{\mu^2}, \alpha(\mu^2) \right)}{c_0 \left(\frac{q^2}{\mu^2}, \alpha(\mu^2) \right)} = 0. \tag{B5}$$

We can proceed in the same way for the ghost dressing function and derive analogous equations for the Wilson coefficients \tilde{c}_i that differ from those for c_i only because $\tilde{\gamma}(\alpha(\mu^2))$ takes the place of $\gamma(\alpha(\mu^2))$. Thus, the combination \tilde{c}_2/\tilde{c}_0 obeys exactly the same Eq. (B5), above derived for c_2/c_0 , that can be solved at the leading logarithm as explained in [8] to give

$$\frac{c_2(\frac{q^2}{\mu^2}, \alpha(\mu^2))}{c_0(\frac{q^2}{\mu^2}, \alpha(\mu^2))} = \frac{\tilde{c}_2(\frac{q^2}{\mu^2}, \alpha(\mu^2))}{\tilde{c}_0(\frac{q^2}{\mu^2}, \alpha(\mu^2))} = 3g^2(q^2) \left(\frac{g^2(q^2)}{g^2(\mu^2)} \right)^{-\gamma_0^{A^2}/\beta_0}. \quad (\text{B6})$$

The boundary condition comes from requiring Eq. (B3) to be equal to Eq. (29) for the ghost and Eq. (32) for the gluon at $\mu^2 = q^2$. The coefficient $\gamma_0^{A^2}$ was computed to be 35/4 for the first time in [8]. Of course, Eqs. (B3) define not only the dependence of the Wilson coefficient on the renormalization momentum μ^2 but also that on the momentum scale q^2 because of standard dimensional arguments: the only dimensionless quantities¹⁰ are the ratio q^2/μ^2 and α .

¹⁰Other dimensionless quantities can be obtained with the help of Λ_{QCD} , but this is a nonperturbative parameter not emerging in the Wilson coefficient dominated by the short-distance singularities of the OPE expansion and only coding perturbative information in the SVZ approach.

Then, putting all together, the nonperturbative formula for the running coupling at the leading logarithm is given by

$$\alpha_T(\mu^2) = \alpha_T^{\text{pert}}(\mu^2) \left(1 + \frac{9}{\mu^2} \left(\frac{\ln \frac{\mu^2}{\Lambda_{\text{QCD}}^2}}{\ln \frac{\mu_0^2}{\Lambda_{\text{QCD}}^2}} \right)^{-9/44} \times \frac{g_T^2(\mu_0^2) \langle A^2 \rangle_{R, \mu_0^2}}{4(N_C^2 - 1)} \right), \quad (\text{B7})$$

where the only correction to Eq. (33) comes from the ratio of logarithms inside the bracket that, as can be seen in Fig. 5, introduces no significant deviation.

-
- [1] G. S. Bali and K. Schilling, *Phys. Rev. D* **47**, 661 (1993).
 - [2] M. Luscher, R. Sommer, P. Weisz, and U. Wolff, *Nucl. Phys.* **B413**, 481 (1994); S. Capitani, M. Luscher, R. Sommer, and H. Wittig (Alpha Collaboration), *Nucl. Phys.* **B544**, 669 (1999).
 - [3] G.M. de Divitiis, R. Frezzotti, M. Guagnelli, and R. Petronzio, *Nucl. Phys.* **B433**, 390 (1995).
 - [4] B. Alles, D. Henty, H. Panagopoulos, C. Parrinello, C. Pittori, and D. G. Richards, *Nucl. Phys.* **B502**, 325 (1997).
 - [5] P. Boucaud, J.P. Leroy, J. Micheli, O. Pene, and C. Roiesnel, *J. High Energy Phys.* 10 (1998) 017.
 - [6] P. Boucaud *et al.*, *J. High Energy Phys.* 04 (2000) 006.
 - [7] Ph. Boucaud, A. Le Yaouanc, J.P. Leroy, J. Micheli, O. Pène, and J. Rodriguez-Quintero, *Phys. Lett. B* **493**, 315 (2000).
 - [8] Ph. Boucaud, A. Le Yaouanc, J.P. Leroy, J. Micheli, O. Pène, and J. Rodriguez-Quintero, *Phys. Rev. D* **63**, 114003 (2001); F. De Soto and J. Rodriguez-Quintero, *Phys. Rev. D* **64**, 114003 (2001).
 - [9] A. Sternbeck, K. Maltman, L. von Smekal, A.G. Williams, E.M. Ilgenfritz, and M. Muller-Preussker, *Proc. Sci., LAT2007* (2007) 256.
 - [10] P. Boucaud *et al.*, *Phys. Rev. D* **66**, 034504 (2002); *J. High Energy Phys.* 04 (2003) 005; *Phys. Rev. D* **70**, 114503 (2004).
 - [11] F.V. Gubarev and V.I. Zakharov, *Phys. Lett. B* **501**, 28 (2001).
 - [12] P. Boucaud, J.P. Leroy, H. Moutarde, J. Micheli, O. Pene, J. Rodriguez-Quintero, and C. Roiesnel, *J. High Energy Phys.* 01 (2002) 046.
 - [13] Ph. Boucaud *et al.* (ETM Collaboration), *Comput. Phys. Commun.* **179**, 695 (2008).
 - [14] J.C. Taylor, *Nucl. Phys.* **B33**, 436 (1971).
 - [15] L. von Smekal, R. Alkofer, and A. Hauck, *Phys. Rev. Lett.* **79**, 3591 (1997).
 - [16] K.G. Chetyrkin and T. Seidensticker, *Phys. Lett. B* **495**, 74 (2000).
 - [17] Ph. Boucaud, J.P. Leroy, A. Le Yaouanc, A. Y. Lokhov, J. Micheli, O. Pene, J. Rodriguez-Quintero, and C. Roiesnel, arXiv:hep-ph/0507104.
 - [18] K.G. Chetyrkin and A. Retey, arXiv:hep-ph/0007088.
 - [19] T. van Ritbergen, J.A.M. Vermaseren, and S.A. Larin, *Phys. Lett. B* **400**, 379 (1997).
 - [20] K.G. Chetyrkin, *Nucl. Phys.* **B710**, 499 (2005).
 - [21] M. Czakon, *Nucl. Phys.* **B710**, 485 (2005).
 - [22] Ph. Boucaud *et al.*, *Phys. Rev. D* **72**, 114503 (2005).
 - [23] D. Dudal, H. Verschelde, and S.P. Sorella, *Phys. Lett. B* **555**, 126 (2003); K.I. Kondo, *Phys. Lett. B* **572**, 210 (2003); arXiv:hep-th/0306195.
 - [24] R. Wilson, *Phys. Rev.* **179**, 1499 (1969).
 - [25] Ph. Boucaud *et al.*, *J. High Energy Phys.* 01 (2006) 037; Ph. Boucaud, A. Le Yaouanc, J.P. Leroy, J. Micheli, O. Pène, and J. Rodriguez-Quintero, *Phys. Rev. D* **63**, 114003 (2001).
 - [26] M.A. Shifman, A.I. Vainshtein, and V.I. Zakharov, *Nucl. Phys.* **B147**, 385 (1979); M.A. Shifman, A.I. Vainshtein, M.B. Voloshin, and V.I. Zakharov, *Phys. Lett.* **77B**, 80 (1978).
 - [27] Ph. Boucaud *et al.*, *Phys. Rev. D* **74**, 034505 (2006).
 - [28] R. Sommer, *Nucl. Phys.* **B411**, 839 (1994).